# An Amphiphilic Trinuclear Cobalt Cluster-containing Molecular Unit: Synthesis, Characterization and Langmuir–Blodgett Films†

**Robert Deschenaux,*[a] Claudio Masoni,[a] Helen Stoeckli-Evans,[a] Sebastien Vaucher,[a] Jürgen Ketterer,[b] Rolf Steiger[a,b] and (the late) Albrecht L. Weisenhorn[c]**

[a] *Université de Neuchâtel, Institut de Chimie, Av. de Bellevaux 51, CH-2000 Neuchâtel, Switzerland*

[b] *Ilford S.A., CH-1723 Marly, Switzerland*

[c] *Université de Fribourg, Institut d'Histologie et d'Embriologie Générale, Pérolles, CH-1700 Fribourg, Switzerland*

An amphiphilic polynuclear transition-metal cluster has been prepared and its capability for forming layers at the air–water interface and Langmuir–Blodgett films on different substrates investigated. The compound was obtained by linking a $Co_3(CO)_9$ cluster to a hydrophobic cholesterol framework. A polar head was introduced by substituting one CO ligand by an isocyanide derivative bearing a hydrophilic functional group. The surface pressure and surface potential *vs.* area isotherms and Brewster-angle microscopy indicated the formation of stable Langmuir films. Up to thirty-six transfers were performed on hydrophobized solids (mica, glass, quartz and silicon wafers). Structural characterization of the transferred films (UV and IR spectroscopy, atomic force microscopy, small-angle X-ray scattering) demonstrated the formation of stable, highly organized crystals. The results represent a novel strategy towards the development of supramolecular assemblies from polynuclear transition-metal compounds and organometallic surfaces. The structure of $[Co_3(CO)_8(CCO_2Me)(CNC_6H_4CN)]$ has been established by X-ray crystallography.

The Langmuir–Blodgett technique is currently the subject of intense investigation:[1] the possibility of fabricating tailor-made supramolecular assemblies, with well defined structures,[2] and of studying specific properties at the molecular level has allowed a better understanding of fundamental phenomena occurring at the frontiers of chemistry, biology and physics.[3] From a practical point of view, this technique could lead to the development of new technologies, such as in the miniaturization of electronic and optical devices (nanometer-scale technology).

Recent studies have shown that a large variety of structures can be used as amphiphiles. Stable monolayers and Langmuir–Blodgett films have been obtained from porphyrins,[4] phthalocyanins,[5] oligothiophenes,[6] polymers,[7] ferrocenes,[8] ruthenium complexes,[9] cyclodextrins,[10] macrocyclic polyamides[11] and calixarenes.[12] This clearly demonstrates the wide scope of the method. The design and the synthesis of new amphiphiles, combining an original and elegant structure with unique properties, constitutes a challenging goal towards the elaboration of new materials based on this technology.

In the present paper we describe the synthesis and characterization of an amphiphilic organometallic cluster derived from a tricobalt core, and demonstrate, for the first time, that polynuclear transition-metal frameworks can be used as molecular units to form stable Langmuir–Blodgett films. The remarkable magnetic,[13] electrochemical[14] and structural[15] features of organometallic clusters motivated us to undertake this research.

## Results and Discussion

*Synthesis.*—The investigated amphiphilic cluster **1** consists of a trinuclear cobalt core connected to a cholesterol (cholest-5-en-3β-ol) moiety, acting as the hydrophobic tail. The nitrile function, introduced by substitution of one CO ligand with an isocyanide derivative, acts as the polar headgroup. The synthesis of **1** is shown in Scheme 1. Treatment of methyl 4-hydroxybenzoate **I** with dimethoxymethane and $P_2O_5$ in $CH_2Cl_2$ gave the protected phenol intermediate **II** (89%), which was transformed into the cholesterol derivative **III** (84%) by transesterification [LiBu, cholesterol, tetrahydrofuran (thf)]. Removal of the protecting group under acidic conditions ($HCl$–$MeCO_2H$, thf) yielded **IV** (85%). Alkylation of the latter with 2-bromoethanol in the presence of $K_2CO_3$ gave **V** (83%). The nonacarbonyltricobalt cluster **2** was prepared, adapting a two-step literature procedure,[16] in 44% yield from **3**[17] and **V**: chloro cluster **3** was first treated with $AlCl_3$ in $CH_2Cl_2$ to produce an acylium intermediate,[17] which was esterified with alcohol **V**. Reaction of **2** with isocyanide **VIII** (thf, room temperature) afforded, after purification by column chromatography (silica gel; hexane–$CH_2Cl_2$–$Et_2O$, 6:2:1) and crystallization from hexane, the targeted cluster **1** (25%). The isocyanide **VIII** was synthesised as depicted in Scheme 2: 4-aminobenzonitrile **IX** was heated in $HCO_2H$ to give **X** (75%), dehydration of which in $POCl_3$–$NHPr^i_2$[18] led to **VIII** (80%) as a white solid.

Compound **VIII** is a potentially bidentate ligand. Its co-ordination to cluster **1** by the isocyanide function is demonstrated by comparing their IR spectra (KBr). Indeed, the wavenumber of the nitrile group is identical for both compounds (2232 $cm^{-1}$ for **VIII** and 2233 $cm^{-1}$ for **1**), while that of the isocyanide function is clearly different: 2133 $cm^{-1}$ for uncoordinated **VIII** and 2152 $cm^{-1}$ for **1**. The observed shift of 19 $cm^{-1}$ results unambiguously from the co-ordination of the isocyanide group.

*Solid-state Structure.*—To understand the behaviour and arrangement of the investigated amphiphile **1** at the air–water interface and within the transferred films its structure must be known. The monosubstitution was confirmed by $^1H$ NMR spectroscopy and elemental analysis. However, the substitution

† *Supplementary data available:* see Instructions for Authors, *J. Chem. Soc., Dalton Trans.*, 1994, Issue 1, pp. xxiii–xxviii.

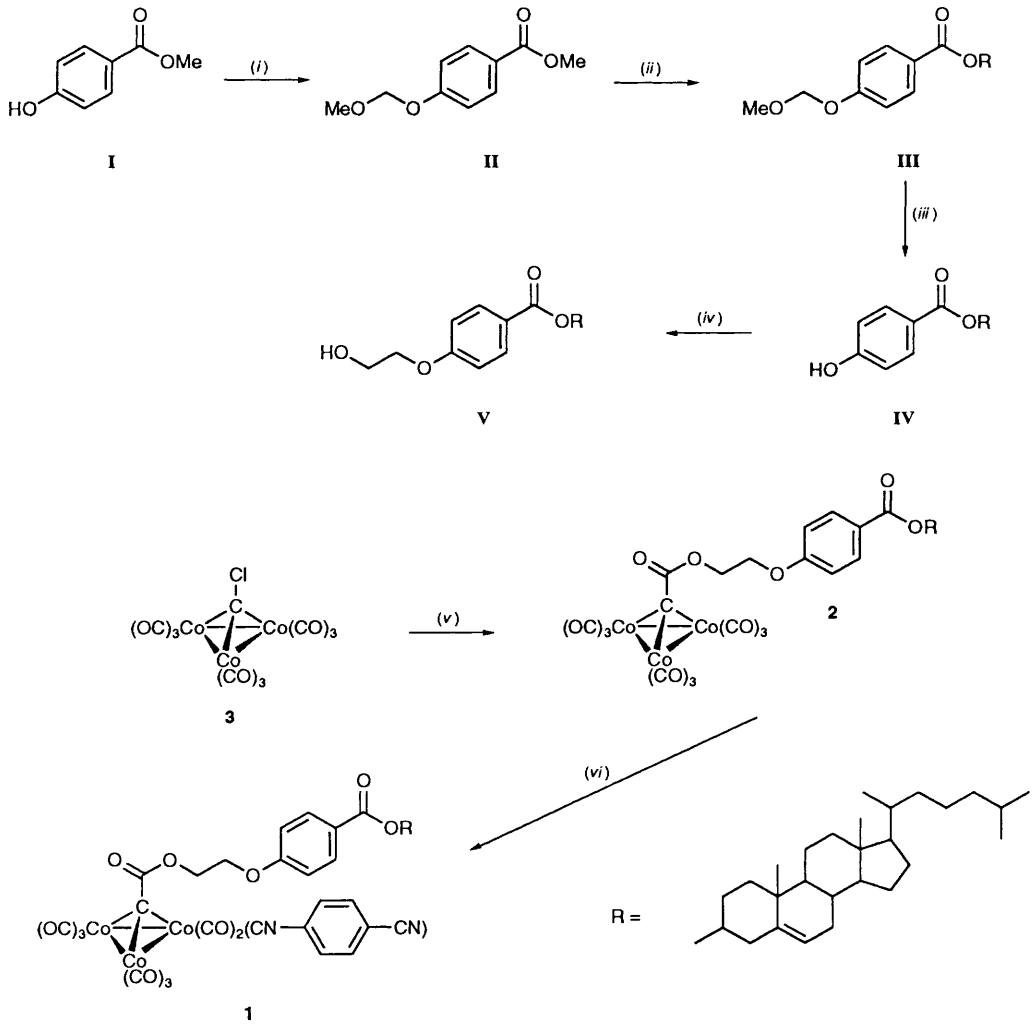

**Scheme 1** (*i*) $CH_2(OMe)_2$, $P_2O_5$, $CH_2Cl_2$, yield 89%; (*ii*) cholesterol, LiBu, thf, 84%; (*iii*) HCl, $MeCO_2H$, thf, 85%; (*iv*) $HOCH_2CH_2Br$, $K_2CO_3$, thf, dmf, 83%; (*v*) (*a*) $AlCl_3$, $CH_2Cl_2$; (*b*) **V**, 44%; (*vi*) **VIII**, thf, 25%

position, *i.e.* equatorial or axial, occupied by the isocyanide ligand, required a crystal structure determination. This point is of crucial importance since equatorial or axial substitution leads to two structures with very different molecular shapes.

So far, all attempts to obtain crystals of cluster **1** suitable for a structure determination have failed. This was attributed to the structural complexity of this material. Therefore, we decided to investigate the structural characterization of the model compound **4**, in which the large organic cholesterol derivative framework was replaced by a methyl group. First, we expected that **4** would crystallize more easily than **1**. Secondly, as clusters **2** and **5** are built from the same nonacarbonyl tricobalt architecture, we anticipated that treatment of either with isocyanide **VIII**, under strictly identical reaction conditions, would lead to the same substitution (see Experimental section). In fact, the solution IR spectra of **1** and **4** gave identical patterns in the CO region. These data provided evidence that in both structures the CO substitution occurred at the same position.

Crystals of cluster **4** suitable for an X-ray structure analysis were obtained from a saturated hexane–$CH_2Cl_2$ solution. The molecular structure and the numbering scheme are presented in Fig. 1. The atomic coordinates and selected bond lengths and angles are collected in Tables 1 and 2, respectively. The crystal structure determination clearly established the equatorial substitution of the isocyanide ligand. The replacement of one equatorial CO ligand by **VIII** did not lead to important structural modifications, and the bond lengths and angles are in agreement, within experimental error, with values reported for either substituted or unsubstituted tricobalt clusters such as

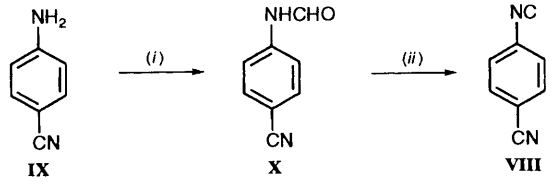

**Scheme 2** (*i*) $HCO_2H$, yield 75%; (*ii*) $POCl_3$, $NHPr^i_2$, $CH_2Cl_2$, 80%

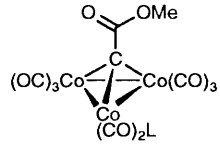

**4** L = **VIII**
**5** L = CO

$[Co_3(CMe)(CO)_9]$:[20] the three cobalt atoms nearly form an equilateral triangle with angles deviating by 0.4° at most from the theoretical value (60°). The mean value of the cobalt–cobalt bond lengths was found to be 0.2473 nm. Identical distances were found between the apical C(1) carbon atom and the cobalt atoms (mean 0.1903 nm). Finally, the length of 0.1141 nm revealed a multiple-bond character for the C(4)–N(1) bond.

*Film Formation at the Air–Water Interface.*—Monolayers were first prepared from the cholesterol derivative **V**. The latter

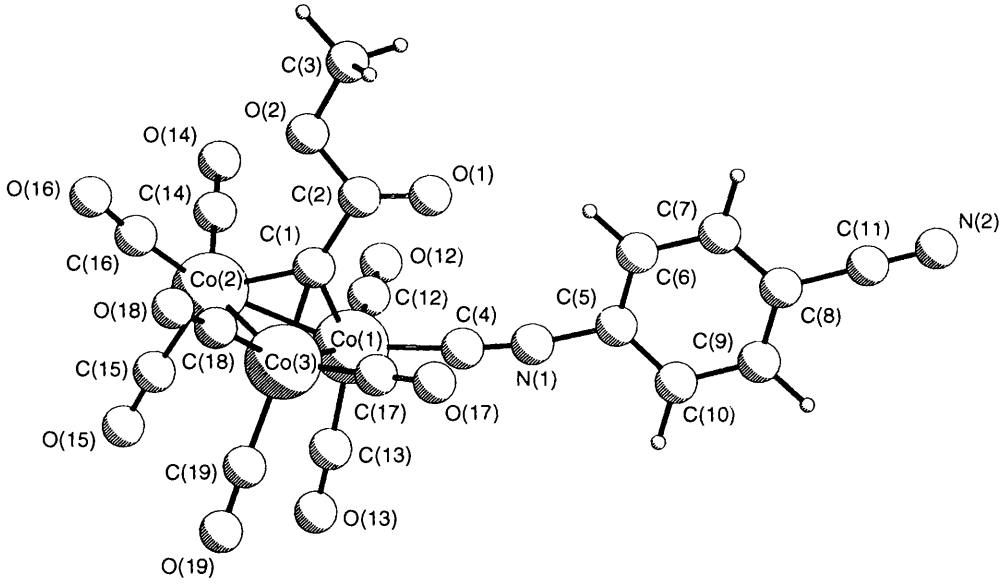


**Fig. 1** A PLUTO[19] plot of cluster **4** showing the arbitrary numbering scheme

**Table 1** Atomic coordinates for cluster **4**

| Atom | *x* | *y* | *z* |
|---|---|---|---|
| Co(1) | 0.013 36(5) | 0.214 62(5) | 0.174 27(3) |
| Co(2) | 0.206 62(6) | 0.022 14(6) | 0.148 92(4) |
| Co(3) | 0.285 84(5) | 0.281 62(5) | 0.117 54(3) |
| C(1) | 0.171 4(4) | 0.137 9(4) | 0.240 5(3) |
| C(2) | 0.174 4(5) | 0.115 8(5) | 0.348 9(3) |
| O(1) | 0.127 3(5) | 0.200 3(5) | 0.396 6(3) |
| O(2) | 0.241 9(5) | −0.015 6(4) | 0.386 3(3) |
| C(3) | 0.252 5(9) | −0.043 3(7) | 0.492 4(4) |
| N(1) | −0.125 5(4) | 0.423 7(4) | 0.294 6(3) |
| N(2) | −0.513 1(6) | 0.721 1(6) | 0.662 4(4) |
| C(4) | −0.068 2(4) | 0.350 4(5) | 0.244 8(3) |
| C(5) | −0.200 2(4) | 0.491 6(4) | 0.369 4(3) |
| C(6) | −0.169 2(6) | 0.441 9(5) | 0.465 3(4) |
| C(7) | −0.247 0(5) | 0.504 2(6) | 0.540 5(4) |
| C(8) | −0.352 5(5) | 0.616 7(5) | 0.518 7(3) |
| C(9) | −0.379 5(5) | 0.667 7(5) | 0.421 7(3) |
| C(10) | −0.302 7(5) | 0.606 1(5) | 0.345 5(3) |
| C(11) | −0.440 6(5) | 0.675 3(6) | 0.598 9(4) |
| C(12) | −0.143 0(5) | 0.086 9(5) | 0.240 0(3) |
| O(12) | −0.241 5(4) | 0.005 3(4) | 0.283 4(3) |
| C(13) | −0.030 9(4) | 0.295 2(4) | 0.049 1(3) |
| O(13) | −0.056 6(4) | 0.340 6(4) | −0.029 5(3) |
| C(14) | 0.095 2(6) | −0.137 7(6) | 0.236 1(5) |
| O(14) | 0.027 9(6) | −0.238 7(5) | 0.294 4(5) |
| C(15) | 0.193 3(6) | 0.037 7(6) | 0.019 8(4) |
| O(15) | 0.177 9(5) | 0.052 7(6) | −0.060 3(3) |
| C(16) | 0.382 2(6) | −0.070 4(6) | 0.161 8(5) |
| O(16) | 0.488 3(5) | −0.136 3(5) | 0.176 6(5) |
| C(17) | 0.269 1(5) | 0.438 8(5) | 0.163 9(3) |
| O(17) | 0.261 3(5) | 0.537 3(4) | 0.194 1(3) |
| C(18) | 0.482 6(5) | 0.239 9(5) | 0.113 6(3) |
| O(18) | 0.607 1(4) | 0.215 0(5) | 0.108 8(4) |
| C(19) | 0.302 1(5) | 0.370 3(5) | −0.021 9(3) |
| O(19) | 0.311 4(5) | 0.423 8(5) | −0.107 07(24) |

**Table 2** Selected bond lengths (nm) and angles (°) for cluster **4**

| | | | |
|---|---|---|---|
| Co(1)–Co(2) | 0.246 43(8) | Co(1)–C(4) | 0.185 8(4) |
| Co(1)–Co(3) | 0.247 21(8) | Co(1)–C(12) | 0.178 9(4) |
| Co(2)–Co(3) | 0.248 30(9) | Co(1)–C(13) | 0.182 2(4) |
| Co(1)–C(1) | 0.190 2(4) | N(1)–C(4) | 0.114 1(5) |
| Co(2)–C(1) | 0.190 0(4) | N(1)–C(5) | 0.139 9(5) |
| Co(3)–C(1) | 0.190 8(4) | N(2)–C(11) | 0.114 1(6) |
| Co(2)–Co(1)–Co(3) | 60.397(24) | C(1)–Co(1)–C(12) | 106.94(17) |
| Co(1)–Co(2)–Co(3) | 59.956(24) | Co(2)–Co(1)–C(12) | 95.78(13) |
| Co(1)–Co(3)–Co(2) | 59.647(21) | Co(3)–Co(1)–C(4) | 100.97(12) |
| C(1)–Co(1)–C(4) | 98.17(17) | | |

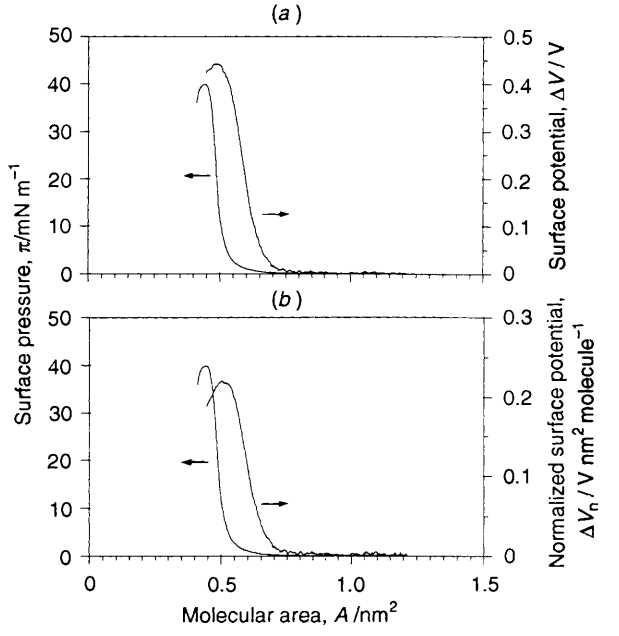


**Fig. 2** Surface pressure *vs.* area isotherms of compound **V** (20.0 °C, aqueous $CdCl_2$–$NaHCO_3$ subphase) with (*a*) surface potential and (*b*) normalized surface potential ($\Delta V_n$ = surface potential × molecular area)

showed the typical behaviour of amphiphiles at the air–water interface. Indeed, the surface pressure and surface potential *vs.* area isotherms (Fig. 2) clearly demonstrated the formation of a stable film at the air–water interface. The limiting area $A_0$ = 0.52 $nm^2$ also confirmed the obtention of a crystalline solid. The results obtained for **V** are in agreement with literature data reported for other cholesterol derivatives.[21]

Organometallic-containing films were prepared by spreading the amphiphile **1** from $CHCl_3$ solutions on different subphases and at different temperatures. The $\pi$ *vs.* *A* isotherms showed that compound **1** formed stable films between 10 and 20 °C on a $CdCl_2$–$NaHCO_3$ solution (Fig. 3) as well as on pure water (Fig. 4). A strong reduction of the collapse pressure, corresponding

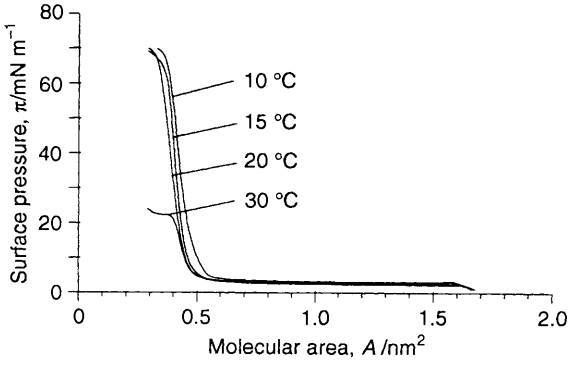


**Fig. 3** Surface pressure *vs.* area isotherms of cluster **1** at different temperatures on an aqueous $CdCl_2$–$NaHCO_3$ subphase

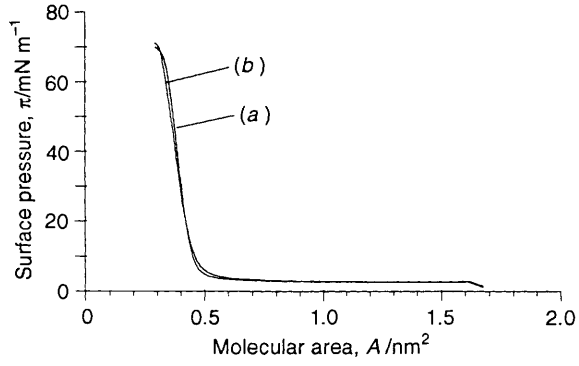


**Fig. 4** Comparison of the surface pressure *vs.* area isotherms of cluster **1** on pure water (*a*) and on aqueous $CdCl_2$–$NaHCO_3$ (*b*) subphases at 20.0 °C

to a decrease in film stability, was observed at 30 °C. At 20 °C a limiting area $A_0 = 0.46$ nm$^2$, which corresponds to approximately half the value calculated from the CSC Chem3D Plus™ models (0.80–0.85 nm$^2$, see Fig. 10), was determined for each subphase. This finding indicated that amphiphile **1** did not organize in a classical monolayer at high surface pressure. Lowering of the temperature affected the limiting area only slightly: $A_0 = 0.47$ and 0.49 nm$^2$ at 15 and 10 °C, respectively.

The surface potentials measured during the compression of cluster **1** (Fig. 5) revealed interesting features and suggested a head-to-tail organization of **1** [see Fig. 12(*b*)]. First, a sharp increase of $\Delta V$, corresponding to the slight increase of the surface pressure, was observed at 1.80 nm$^2$. This result was attributed to the formation of a monolayer of low stability (5 mN m$^{-1}$). Secondly, the regular decrease of the normalized surface potential [Fig. 5(*b*)], upon further compression, while the surface pressure remained constant (plateau), clearly indicated the transformation of the monolayer into a new structure in which the molecular units of **1** must be arranged in such a way as to produce an assembly with a low overall dipole moment. This situation is achieved when the molecular units of **1** are associated in pairs with the tricobalt cluster cores pointing in opposite directions, *i.e.* in a head-to-tail arrangement, which confirms the $A_0$ values obtained from the $\pi$ *vs.* $A$ isotherms.

Brewster-angle microscopy[22] (BAM) was used to visualize the phenomena occurring at the air–water interface. Fig. 6 shows photomicrographs at different stages during the compression of cluster **1** on a $CdCl_2$–$NaHCO_3$ subphase at 20 °C. Similar observations were obtained on pure water. Highly reflectant circular domains appeared at 1.60 nm$^2$, the size and number of which increased upon compression in the plateau region [Fig. 6(*a*) and 6(*b*)]. From 0.50 nm$^2$, *i.e.* during the increase of the surface pressure, the circular domains approached each other and assembled to produce a uniform surface [Fig. 6(*c*)]. The collapse of the latter is presented in Fig. 6(*d*). Several hysteresis curves were recorded between 0 and 60

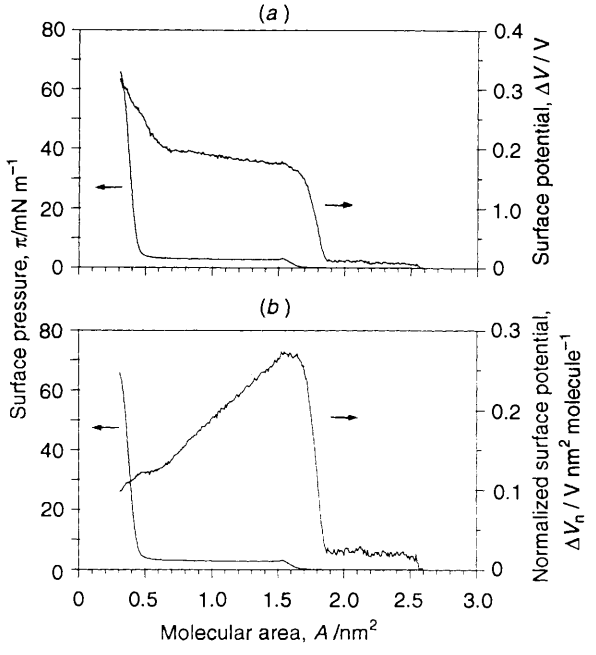


**Fig. 5** Surface pressure *vs.* area isotherms of cluster **1** (20.0 °C, aqueous $CdCl_2$–$NaHCO_3$ subphase) with (*a*) surface potential and (*b*) normalized surface potential

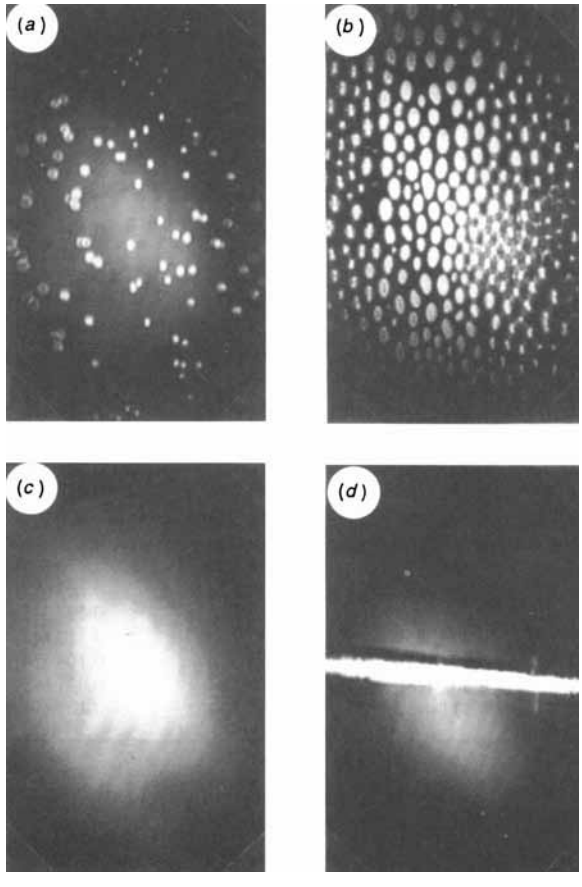


**Fig. 6** Brewster-angle microscopy during the compression of cluster **1** [see Fig. 5(*b*), for example]: circular domains at (*a*) 1.5 and (*b*) 0.8 nm$^2$; (*c*) homogeneous Langmuir film at 0.41 nm$^2$ (20 mN m$^{-1}$) (interference fringes are always visible); (*d*) collapse at 0.30 nm$^2$. The images are untreated; owing to the angle of the reflected laser beam [23b] the domains appear as ellipsoids

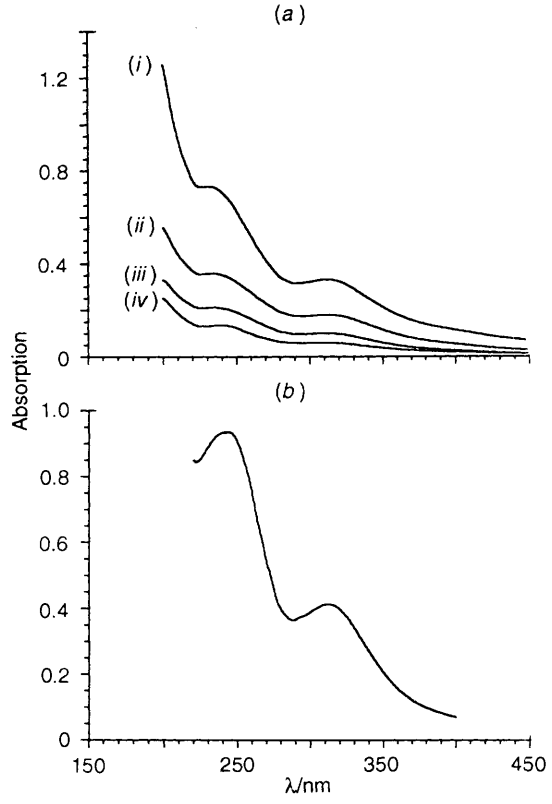


**Fig. 7** The UV spectra of cluster **1** transferred onto quartz plates (*a*) and in $CH_2Cl_2$ solution ($1.60 \times 10^{-4}$ mol $dm^{-3}$) (*b*). Number of layers in (*a*): 32 (*i*), 16 (*ii*), 8 (*iii*) and 4 (*iv*)

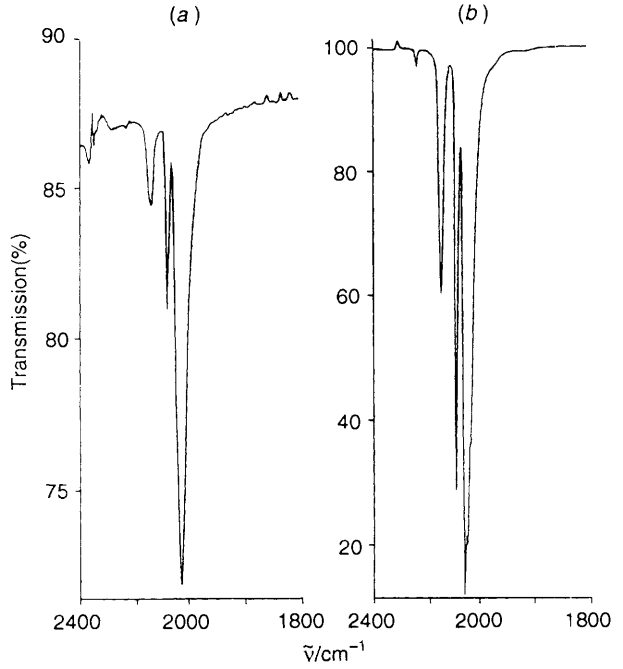


**Fig. 8** The IR spectra of cluster **1** transferred onto a silicon wafer (12 transfers, 50 FTIR scans) (*a*) and in $CH_2Cl_2$ solution (*b*)

mN $m^{-1}$. In each case, identical $\pi$ *vs.* *A* isotherms and BAM images were obtained, demonstrating the reversibility of the overall process.

A detailed interpretation of the above images cannot be given due to the lack of literature data. So far, only fatty acids,[23] phospholipids,[22a] and more recently a smectic liquid crystalline polymer[24] have been studied by means of BAM during the formation of mono- and/or multi-layers at the air–water interface. In the present study, BAM demonstrated unequivocally the formation of a regular and compact film at 0.46 $nm^2$, and confirmed visually the capability of cluster **1** to organize at the air–water interface. In addition, the evolution of the BAM images, with respect to the $\pi$ and $\Delta V$ *vs.* *A* isotherms, seems to indicate that the head-to-tail organization of **1** starts from the bright circular domains, the assembling of which leads to the Langmuir films at 0.46 $nm^2$.

*Y-Type Transferred Films.*—Langmuir–Blodgett films were prepared using the conventional dipping method (see Experimental section). The Y-transfer mode (downward and upward deposition) was successfully applied onto different hydrophobized substrates (quartz, glass, mica, silicon wafer) and in each case a transfer ratio ($T_R$) close to unity was obtained. The transferred films were characterized by means of UV and IR spectroscopy, atomic force microscopy (AFM) and small-angle X-ray scattering (SAXS).

(*a*) *UV and IR spectroscopy.* Films were deposited onto quartz plates (UV) and silicon wafers (IR), both pretreated with $SiMe_2Cl_2$. The UV and IR spectra of the transferred films are identical to those of cluster **1** in solution (Figs. 7 and 8). The UV absorption of the transferred films increased linearly with the number of layers. The chemical stability of the transferred films was evaluated by measuring the variation of the absorption maximum as a function of time. Only a slight decrease of the absorption (about 5%) was detected after 3 weeks, which indicated a good chemical stability of the deposited layers.

(*b*) *Atomic force microscopy.* Structural properties of films built up from cluster **1** were investigated by means of AFM. This technique[25] was successfully applied to image films, obtained from either amphiphilic[26] or hydrophobic[27] compounds, with molecular resolution.

Two AFM images of five-layer films, transferred onto silicon wafers silanized with $SiMe_2Cl_2$, are presented in Fig. 9. At low magnification [Fig. 9(*a*)] a long-range crystalline ordering of the films is observed. Calculations from the Fourier spectrum gave repeat distances of 0.96 ± 0.05 and 0.95 ± 0.02 nm in the 25 ± 2 and 103 ± 3° directions (measured from the positive *x* axis). From these values the area of a unit cell is found to be 0.88 ± 0.06 $nm^2$. At a higher magnification [Fig. 9(*b*)] the same values were obtained (within 5%) with the Fourier spectrum showing again the peaks of a periodic structure. Therefore the crystalline structure of the films was confirmed both at low and high magnification.

The cell dimensions calculated by AFM are consistent with the molecular dimensions obtained from the CSC Chem3D Plus™ models. The molecular organization of cluster **1**, viewed from the cyano group, is presented in Fig. 10, which images a portion of the surface of the film. Such an arrangement represents a two-dimensional rhombohedric system.

(*c*) *Small-angle X-ray scattering.* The SAXS experiments were carried out on powders of compounds **1**, **V** and **5** and on films of **1** deposited on glass slides hydrophobized with $SiMe_2Cl_2$.

The results for powders of amphiphilic tricobalt cluster **1** showed a well defined diffraction peak at 3.00 ± 0.05 nm. The same value, but with lower intensity, was found, within experimental error, for the cobalt cluster-free cholesterol derivative **V**. In both cases, wide-angle X-ray scattering (WAXS) results indicated that the peak at 3.0 nm arose from reflections generated by unit cells of monoclinic symmetry. Further studies are planned to estimate the crystal structure of **1** *via* Rietveld refinement of powder data to complete the interpretation of the diffraction peaks. The distance of 3.0 nm corresponds notably to the length of compound **V** as determined from Corey–Pauling–Koltun (CPK) molecular models. The tricobalt cluster **5**, which does not contain the

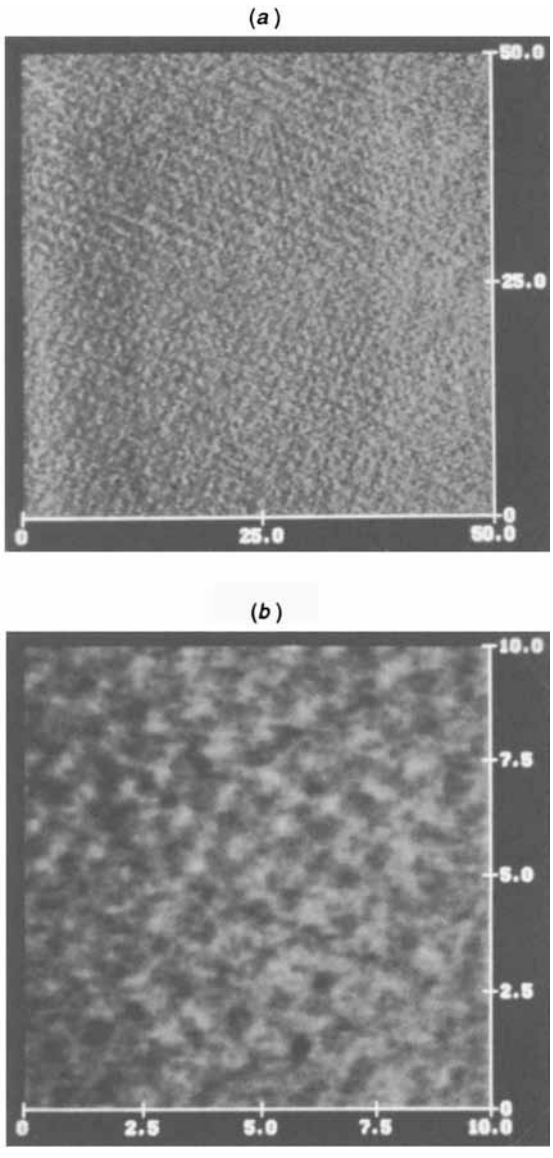


**Fig. 9** The AFM images of a five-layer Langmuir–Blodgett film of cluster **1** (low areas are dark, high areas are light) at (*a*) low (image size 50 × 50 nm, height 0.5 nm) and (*b*) high (image size 10 × 10 nm, height 0.4 nm) magnification. Both scales in nm

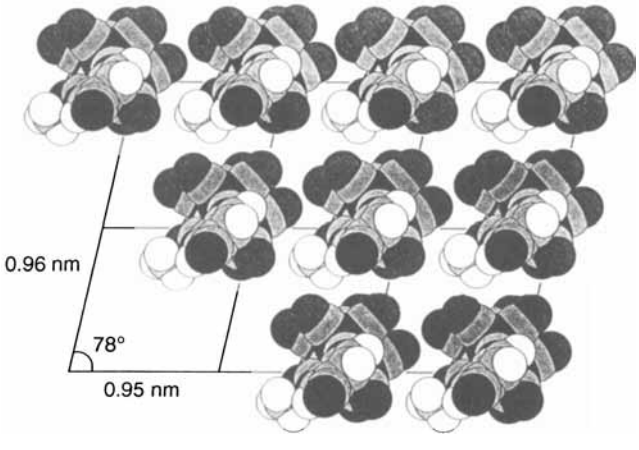


**Fig. 10** Proposed molecular organization of cluster **1** of the film surface according to the rhombohedric system provided by the AFM images (viewed from the nitrile group)

cholesterol framework, exhibited no diffraction signal. Furthermore, analysis of the powders by WAXS showed increased disorder and imperfection with increased structural complexity.

The SAXS structure of Langmuir–Blodgett films showed a sharp and intense peak at 6.0 ± 0.1 nm and a much smaller one at 3.1 nm (Fig. 11). The periodicity of 6.0 nm was attributed to the distance between two tricobalt cluster frameworks in the head-to-tail multilayer structure presented in Fig. 12(*b*). The distance of 3.1 nm, which can be explained by second-order reflection of the periodicity of 6.0 nm, corresponds approximately to the length of the cholesterol derivative [2.9 nm, see Fig. 12(*a*)], as already noted for the powder analyses. The SAXS

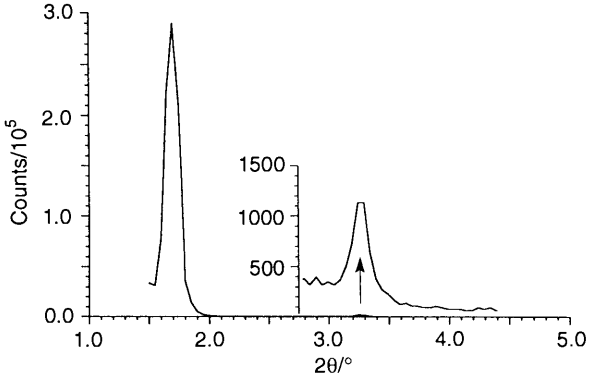


**Fig. 11** Small-angle X-ray scattering of a 18-layer film of cluster **1** on a hydrophobic glass plate. High-intensity peak: 2θ = 1.70° (*d* = 6.02 nm). Weak intensity peak (insert): 2θ = 3.27° (*d* = 3.13 nm)

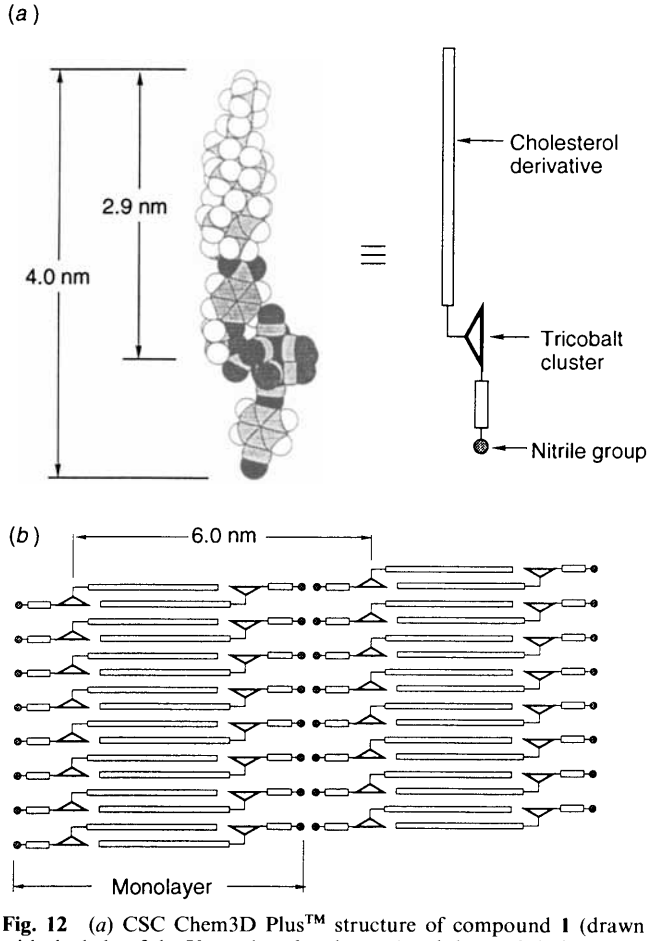


**Fig. 12** (*a*) CSC Chem3D Plus™ structure of compound **1** (drawn with the help of the X-ray data for cluster **4** and those of cholest-5-en-3β-yl *p*-ethoxybenzoate)[28] as well as a symbolic representation. (*b*) Representation of a bilayer film showing the head-to-tail organization of molecular unit **1** within each monolayer; the distance 6.0 nm was observed from SAXS measurements (see text for further details)

results could only be interpreted from ⩾12 layers. Indeed, less than 12 layers gave films of low stability, the structure of which was lost within a few hours at room temperature.

The SAXS results conclusively demonstrated that highly ordered films were obtained from cluster **1**. The head-to-tail structure was observed for all multilayers containing at least 12 layers. The latter were stable for many weeks at room temperature.

*Additional Transfer Experiments.*—The particular structure of the Langmuir–Blodgett films [see Fig. 12(*b*)] prompted us to perform other types of transfers. These preliminary experiments, carried out under identical conditions (20 °C, aqueous $CdCl_2$–$NaHCO_3$ subphase), are described below.

(*a*) A Y-type structure onto a hydrophobic substrate (glass treated with $SiMe_2Cl_2$) could also be obtained ($T_R \approx 1$) starting from an upward deposition.

(*b*) Films of cluster **1** were prepared onto a hydrophobic glass ($SiMe_2Cl_2$) using the X-type transfer mode (downward deposition). A 12-layer film was obtained with excellent transfer ratios ($T_R \approx 1$). Obviously, if head-to-tail layers are transferred, the X- and Y-deposited films should have the same structure. However, it is important to mention that the experimental procedure applied in these two different processes may influence the film organization (during the X-transfer mode the coated plates are allowed to dry before subsequent deposition).

(*c*) One monolayer could be deposited onto a hydrophilic glass plate by lifting up the substrate from the subphase ($T_R \approx 1$). However, the subsequent dipping caused a quantitative return of the transferred monolayer into the floating film.

These results strengthen the evidence for the film structure illustrated in Fig. 12(*b*). First, experiments (*a*) and (*b*) are in agreement with the head-to-tail molecular organization within the monolayer. Secondly, related to (*a*) and (*b*), experiment (*c*) points out the amphiphilic nature of the monolayer surface. Nevertheless, the molecular organization of the first monolayer as well as its interaction with the solid substrates are still unknown. X-Ray measurements have shown that films constituted of few monolayers do not exhibit a well defined structure. The head-to-tail organization presented in Fig. 12(*b*) takes shape during the increasing number of transfers. Ongoing research to elucidate the remaining questions is in progress.

## Conclusion

Stable layers at the air–water interface and ordered Langmuir–Blodgett films were successfully obtained from an amphiphilic tricobalt cluster derivative. The supramolecular organization of the tricobalt cluster-containing molecular unit was carefully investigated by means of surface pressure and surface potential *vs.* area isotherms, Brewster-angle and atomic force microscopy and small-angle X-ray scattering. The postulated head-to-tail structure is consistent with all the data obtained from the above experimental techniques.

The major interest of the work described herein consists of the possibility to design and synthesise organometallic solids and surfaces from the organization of polynuclear transition metal-containing building blocks. Such organometallic assemblies might exhibit new magnetic, electrochemical and optical properties. They could also be used in heterogeneous catalytic reactions and to investigate new substrate–adsorbate interactions in solid–gas adsorption processes (chemical adsorption of CO).

## Experimental

*General.*—Clusters **3**[17] and **5**[16] were prepared according to literature procedures. All other chemicals were used as received without further purification. Thermal properties of cholesterol derivatives **III**–**V** will be reported elsewhere. Column chromatography: silica gel 60 (0.063–0.200 mm, Merck). TLC: silica gel plates 60 $F_{254}$ (Merck). Melting points: Büchi 510 instrument (uncorrected). α: Perkin Elmer 241 polarimeter. UV spectra: Uvikon 930 spectrophotometer. IR spectra: Perkin Elmer 1720 FTIR spectrometer. $^1H$ and $^{13}C$ NMR spectra: Bruker AMX 400 spectrometer at 400.13 MHz ($^1H$) and 100.62 MHz ($^{13}C$); $SiMe_4$ as internal reference; L refers to co-ordinated compound **VIII**. Mass spectra (chemical ionization, $NH_3$): Nermag R 30.10 spectrometer. Program CSC Chem 3D Plus™: Cambridge Scientific Computing, USA.

*Crystal Structure Determination of Cluster* **4**.—$C_{19}H_7Co_3N_2O_{10}$, $M_r = 600.1$, triclinic, space group $P\bar{1}$, $a = 9.165(2)$, $b = 9.455(2)$, $c = 14.107(2)$ Å, $\alpha = 70.69(1)$, $\beta = 73.78(1)$, $\gamma = 84.83(1)°$, $U = 1107.7$ Å$^3$, $Z = 2$, $D_c = 1.799$ g cm$^{-3}$, $\lambda = 0.710\,73$ Å, $\mu = 22.7$ cm$^{-1}$, $F(000) = 594$.

3899 Unique reflections, 3245 observed [$I > 3\sigma(I)$], $R = 0.046$, $R' = 0.067$, $k = 0.002$, $S = 1.40$. Maximum shift/error ratio 0.005 : 1, residual density (e Å$^{-3}$) maximum 0.74, minimum −1.19.

Intensity data were collected at room temperature on a Stoe AED2 four-circle diffractometer using Mo-Kα graphite-monochromated radiation. The structure was solved by Patterson and Fourier difference syntheses using the NRCVAX[29] system, which was used for all further calculations. Neutral complex-atom scattering factors used in NRCVAX[29] were from ref. 30. The H atoms were included in calculated positions [$U_{iso} = U_{eq}(C) + 0.01$ Å$^2$] and renewed after every third cycle of refinement. The non-hydrogen atoms were refined anisotropically using weighted full-matrix least squares, where $w = 1/[\sigma^2(F_o) + k(F_o^2)]$. The numbering scheme used is apparent from Fig. 1, drawn using the program PLUTO.[19]

Additional material available from the Cambridge Crystallographic Data Centre comprises H-atom coordinates, thermal parameters and remaining bond lengths and angles.

*Langmuir–Blodgett Technique.*—Instrumentation: KSV Instrument Inc., Finland. Experiments were carried out on a Langmuir trough LB 5000 (Teflon™ coating, dimensions: 50 × 15 cm) equipped with two hydrophobic barriers, a Wilhelmy balance as a surface-pressure sensor, a film-deposition system and a 5000 SP surface-potential meter (vibrating capacitor method). The whole system, fully computer controlled, lay on an active vibration-isolating table and was protected from dust by a home-made plastic cover.

Measurements of π *vs.* *A* isotherms were carried out by the ordinary method. Typical conditions were as follows: subphase, water (18 MΩ cm$^{-1}$; Elgastat UHQ-II, Kleiner, Switzerland) or aqueous $CdCl_2$ ($1.5 \times 10^{-4}$ mol dm$^{-3}$) and $NaHCO_3$ ($5 \times 10^{-5}$ mol dm$^{-3}$) solution; temperature, subphase thermostatted within ±0.2 °C, atmosphere at 20–22 °C; concentration and volume of chloroform solution of the amphiphile, 1 g dm$^{-3}$, 60–100 mm$^3$; compression speed, 30 cm$^2$ min$^{-1}$. Vertical transfers were performed under the following conditions: subphase, aqueous $CdCl_2$ ($1.5 \times 10^{-4}$ mol dm$^{-3}$) and $NaHCO_3$ ($5 \times 10^{-5}$ mol dm$^{-3}$) solution maintained at 20.0 ± 0.2 °C; deposition surface pressure, 20 mN m$^{-1}$; deposition speed, 0.5 cm min$^{-1}$.

*Brewster-angle Microscopy.*—Instrumentation: BAM-1 Brewster-angle microscope (Nanofilm Technologie, Germany). A detailed description of the instrument was recently published.[23b]

*Atomic Force Microscopy.*—Instrumentation: Nanoscope II AFM (Digital Instruments, USA). Procedure: five layers of cluster **1** were transferred onto a previously silanized ($SiMe_2Cl_2$) ultraflat silicon wafer (Si{100}; Faselec, Switzerland). The next day the wafer was glued to a steel plate and set up into the contact atomic force microscope. Imaging was done

in water with a scanner of 14 μm range and with a short Olympus tip. Only spike removal and low-pass filtering were applied to the images. The AFM analysis of the silanized silicon wafers gave no structure. Further details can be found elsewhere.[27]

*Small-angle X-Ray Scattering*.—All measurements were performed using the Stoe-Stadi P powder diffractometer system. Focused Co-K$\alpha_1$ radiation with $\lambda = 0.178\,898$ nm was obtained by a curved Ge(111) monochromator. The powered samples were investigated in transmission mode with a rotating-sample holder to minimize preferred orientation of the plate-like crystallites. Data were collected with a linear position-sensitive detector (Stoe) in the 1.5–7° (2θ) range (and up to 120° for wide-angle X-ray scattering).

The SAXS results for Langmuir–Blodgett films were recorded using a sample holder for reflection mode in the 2θ range 0.5–5° in combination with a scintillation counter at 130 mm from the sample and with a scan width of 0.02°. The instrument was carefully adjusted by measuring multilayers of cadmium eicosanoate from which good agreement with published data could be achieved.

*Syntheses*.—*Methyl 4-methoxymethoxybenzoate* **II**. Dimethoxymethane (75.2 g, 1.00 mol) and $P_2O_5$ (28.0 g, 0.20 mol) were added to methyl 4-hydroxybenzoate **I** (15.0 g, 0.10 mol) in dry $CH_2Cl_2$ (400 $cm^3$). The mixture was stirred at room temperature overnight, filtered and evaporated. The residue was dissolved in $Et_2O$ (300 $cm^3$) and the ether phase was washed with saturated aqueous $Na_2CO_3$ and saturated aqueous NaCl, dried over $MgSO_4$ and evaporated. The residue was purified by column chromatography ($MeCO_2Et$–hexane, 1:5) to afford compound **II** (17.50 g, 89%) as a colourless *liquid*, $R_f$ ($MeCO_2Et$–hexane, 1:1) 0.52 (Found: C, 61.1; H, 6.3. $C_{10}H_{12}O_4$ requires C, 61.2; H, 6.2%); $\nu_{max}(CH_2Cl_2)$ 2985–2831, 1733 and 1607 $cm^{-1}$; $\delta_H(CDCl_3)$ 3.48 (3 H, s, $OCH_3$), 3.88 (3 H, s, $CO_2CH_3$), 5.22 (2 H, s, $OCH_2O$), 7.05 (2 H, d, aromatic H) and 7.98 (2 H, d, aromatic H).

*Cholest-5-en-3β-yl 4-methoxymethoxybenzoate* **III**. Butyllithium (1.6 mol $dm^{-3}$ in hexane, 100 $cm^3$) was added dropwise, under $N_2$, to a solution of cholesterol (59.1 g, 0.15 mol) in dry thf (150 $cm^3$). The mixture was stirred at 0 °C for 15 min. A solution of methyl ester **II** (15.0 g, 0.08 mol) in dry thf (100 $cm^3$) was added dropwise and the mixture was stirred at room temperature overnight and evaporated. The residue was dissolved in $Et_2O$ (700 $cm^3$) and the organic phase was washed with saturated aqueous NaCl (3 × 200 $cm^3$), dried ($MgSO_4$) and evaporated. The residue was purified by column chromatography ($MeCO_2Et$–hexane, 1:6) to give compound **III** (35.10 g, 84%) as a white *solid*, $R_f$ ($MeCO_2Et$–hexane, 1:1) 0.68, $\alpha$ −4.7° (589.3 nm, 22 °C, $c$ 4.27 × $10^{-2}$ g $cm^{-3}$, $CHCl_3$) (Found: C, 78.5; H, 9.9. $C_{36}H_{54}O_4$ requires C, 78.5; H, 10.0%); $\nu_{max}$(KBr) 2945–2866, 1717, 1607 and 1275 $cm^{-1}$; $\delta_H(CDCl_3)$ 0.69–2.44 (43 H, cholesteryl), 3.48 (3 H, s, $OCH_3$), 4.82 (1 H, m, CHO, cholesteryl), 5.23 (2 H, s, $OCH_2O$), 5.42 (1 H, m, C=CH, cholesteryl), 7.05 (2 H, d, aromatic H) and 7.98 (2 H, d, aromatic H); chemical ionization (CI) mass spectrum $m/z$ 552 ([$M^+$ +2], 1), 369 (86), 368 (100), 353 (18), 283 (2), 247 (10), 213 (14), 165 (37), 147 (60) and 121 (37%).

*Cholest-5-en-3β-yl 4-hydroxybenzoate* **IV**. A mixture of compound **III** (3.70 g, 6.64 mmol), $MeCO_2H$ (100 $cm^3$), 37% aqueous HCl (10 $cm^3$) and thf (70 $cm^3$) was stirred at room temperature for 8 h. The desired product, which precipitated during the reaction, was filtered off and washed with thf (2 × 20 $cm^3$) to afford compound **IV** (2.88 g, 85%) which was used in the following step without further treatment. Purification by column chromatography ($Et_2O$–$CH_2Cl_2$–hexane, 1:15:8) followed by two crystallizations from toluene gave analytically pure **IV**, $R_f$ ($Et_2O$–hexane, 2:1) 0.43, $\alpha$ −6.3° (589.3 nm, 23 °C, $c$ 0.40 × $10^{-2}$ g $cm^{-3}$, $CHCl_3$) (Found: C, 80.6; H, 9.9. $C_{34}H_{50}O_3$ requires C, 80.4; H, 9.9%); $\nu_{max}$(KBr) 3383, 2950–2866, 1711, 1608, 1274 and 1242 $cm^{-1}$; $\delta_H(CDCl_3)$ 0.68–2.45 (43 H, cholesteryl), 4.81 (1 H, m, CHO, cholesteryl), 5.30 (1 H, s, OH), 5.42 (1 H, m, C=CH, cholesteryl), 6.86 (2 H, d, aromatic H) and 7.97 (2 H, d, aromatic H).

*Cholest-5-en-3β-yl 4-(2-hydroxyethoxy)benzoate* **V**. A mixture of phenol **IV** (2.00 g, 3.75 mmol), 2-bromoethanol (1.41 g, 11.3 mmol) and $K_2CO_3$ (1.56 g) in dry dimethylformamide (dmf) (80 $cm^3$) and dry thf (50 $cm^3$) was stirred at 120 °C for 14 h. Additional 2-bromoethanol (1.41 g, 11.3 mmol) and $K_2CO_3$ (1.56 g) were added, and the mixture stirred at 120 °C for 3 h. After cooling to room temperature, $K_2CO_3$ was filtered off and the solution evaporated. The residue was purified by column chromatography ($Et_2O$–$CH_2Cl_2$–hexane, 2:1:1) to give compound **V** (1.71 g, 83%) as a white *solid*, $R_f$ ($Et_2O$) 0.34, $\alpha$ −3.4° (589.3 nm, 22 °C, $c$ 4.41 × $10^{-2}$ g $cm^{-3}$, $CHCl_3$) (Found: C, 78.5; H, 9.9. $C_{36}H_{54}O_4$ requires C, 78.5; H, 9.9%); $\nu_{max}$(KBr) 3543, 2954–2867, 1712, 1609, 1384 and 1276 $cm^{-1}$; $\delta_H(CDCl_3)$ 0.69–2.45 (43 H, cholesteryl), 3.98 (2 H, m, $HOCH_2CH_2O$), 4.14 (2 H, t, $HOCH_2CH_2O$), 4.83 (1 H, m, CHO, cholesteryl), 5.41 (1 H, m, C=CH, cholesteryl), 6.93 (2 H, d, aromatic H) and 8.00 (2 H, d, aromatic H); CI mass spectrum $m/z$ 386 (4), 369 (35), 368 (48), 353 (7), 247 (9), 213 (8), 165 (47), 147 (39) and 121 (100%).

*Cluster* **2**. Freshly sublimed $AlCl_3$ (1.26 g, 9.45 mmol) was added, under $N_2$, to a solution of $[Co_3(CCl)(CO)_9]$ **3** (1.50 g, 3.15 mmol) in dry $CH_2Cl_2$. After stirring at room temperature for 30 min the mixture, initially purple, turned brown and a precipitate formed; TLC (hexane) indicated complete consumption of **3**. Compound **V** (1.56 g, 2.84 mmol) was added. The purple solution was stirred for 10 min and evaporated. The residue was dissolved in $Et_2O$ (200 $cm^3$) and the ether phase was washed twice with 5% aqueous HCl, dried ($MgSO_4$) and evaporated. The solid residue was purified by column chromatography ($CH_2Cl_2$–hexane, 1:1) and crystallized from hexane at −20 °C to give the tricobalt cluster **2** (1.27 g, 44%) as a purple *solid*, $R_f$ ($Et_2O$–hexane, 1:1) 0.54, m.p. 156 °C (decomp.) (Found: C, 55.8; H, 5.2. $C_{47}H_{53}Co_3O_{14}$ requires C, 55.4; H, 5.2%); $\nu_{max}(CH_2Cl_2)$ 2111w, 2065vs and 2047s $cm^{-1}$; $\delta_H(CDCl_3)$ 0.69–2.44 (43 H, cholesteryl), 4.29 (2 H, t, $CO_2CH_2CH_2O$), 4.67 (2 H, t, $CO_2CH_2CH_2O$), 4.81 (1 H, m, CHO, cholesteryl), 5.41 (1 H, m, C=CH, cholesteryl), 6.87 (2 H, d, aromatic H) and 7.98 (2 H, d, aromatic H); $\delta_C(CDCl_3)$ 64.27 ($OCH_2$), 66.70 ($OCH_2$), 114.57 (2 C, aromatic CH), 124.42 (aromatic $CCO_2$), 132.24 (2 C, aromatic CH), 162.73 (aromatic CO), 166.35 ($CO_2$ of cholesteryl), 179.40 ($CO_2CH_2$), 199.17 (9 C, CO), 252.06 ($CCo_3$) and 12.56, 19.42, 20.06, 21.76, 23.24, 23.49, 24.53, 24.99, 28.64, 28.70, 28.92, 32.63, 32.65, 36.49, 36.89, 37.36, 37.76, 38.98, 40.22, 40.46, 43.03, 50.77, 56.86, 57.41, 74.97, 123.37 and 140.45 (27 C, cholesteryl).

*4-Formylaminobenzonitrile* **X**. A mixture of 4-aminobenzonitrile **IX** (5.00 g, 0.042 mol) and $HCO_2H$ (30 $cm^3$) was heated at reflux for 3 h. After cooling to room temperature the solution was evaporated. Recrystallization of the residue from water (100 $cm^3$) afforded 4-formylaminobenzonitrile **X** (4.63 g, 75%) as a white solid m.p. 189 °C (lit.,[31] 188–189 °C); $\nu_{max}$(KBr) 3320–2800, 2223, 1703, 1608, 1523 and 1494 $cm^{-1}$.

*4-Isocyanobenzonitrile* **VIII**. The compound $POCl_3$ (4.18 g, 0.027 mol) was added dropwise, under $N_2$, to a mixture of 4-formylaminobenzonitrile **X** (3.65 g, 0.025 mol), dry diisopropylamine (6.82 g, 0.067 mol) and dry $CH_2Cl_2$ (100 $cm^3$), cooled to 0 °C. The mixture was stirred at 0 °C for 1 h and at room temperature for 14 h. A solution of $Na_2CO_3$ (4.9 g, 0.046 mol) in water (30 $cm^3$) was added dropwise, and the mixture stirred for 1 h. Dichloromethane (50 $cm^3$) was added and the organic phase separated, washed with saturated aqueous $NaHCO_3$ and saturated aqueous NaCl, dried ($MgSO_4$) and evaporated. The residue was purified by column chromatography ($CH_2Cl_2$) to give 4-isocyanobenzonitrile **VIII** (2.60 g, 80%) as a white, bad-smelling solid, $R_f$ ($CH_2Cl_2$) 0.60, m.p. 129 °C (decomp.) (lit.,[32] 130 °C) (Found: C, 74.5; H, 3.2; N, 21.75. Calc. for $C_8H_4N_2$: C, 75.0; H, 3.15; N, 21.85%); $\nu_{max}$(KBr) 3096, 3048, 2232, 2133,

1605 and 1500 $cm^{-1}$; $\delta_H(CDCl_3)$ 7.50 (2 H, d, aromatic H) and 7.73 (2 H, d, aromatic H); $\delta_C(CDCl_3)$ 113.46 ($C^1$), 117.12 (PhCN), 127.27 (3 C, $C^{3-5}$), 133.50 (2 C, $C^{2,6}$) and 169.20 (PhNC).

*Cluster* **1**. Isocyanide **VIII** (63 mg, 0.49 mmol) was added, under $N_2$, to a solution of cluster **2** (200 mg, 0.20 mmol) in dry thf (15 $cm^3$). The mixture was stirred at room temperature for 5 h, filtered through a short silica gel column and eluted with $CH_2Cl_2$. The mixture was evaporated and the residue submitted to column chromatography (hexane–$CH_2Cl_2$–$Et_2O$, 6:2:1) to separate unreacted **2** (35%), which eluted first, followed by cluster **1** (27%) and then by polysubstituted clusters. Recrystallization at −20 °C afforded pure **1** (55 mg, 25%) as a purple *solid*, $R_f$ ($Et_2O$–hexane, 1:1) 0.40, m.p. < 50 °C (decomp.) (Found: C, 57.75; H, 5.05; N, 2.55. $C_{54}H_{57}Co_3N_2O_{13}$ requires C, 58.0; H, 5.1; N, 2.5%); $\lambda_{max}$/nm ($\varepsilon$/$dm^3$ $mol^{-1}$ $cm^{-1}$) ($CH_2Cl_2$) 243 (58 300), 312 (25 800) and 540 (1900); $\nu_{max}(CH_2Cl_2)$ 2235m, 2142s, 2087vs and 2054 (sh); (KBr) 3000–2800, 2233, 2152, 2092, 2045, 1708, 1673 and 1604 $cm^{-1}$; $\delta_H(CDCl_3)$ 0.66–2.46 (43 H, cholesteryl), 4.27 (2 H, t, $CO_2CH_2CH_2O$), 4.65 (2 H, t, $CO_2CH_2CH_2O$), 4.82 (1 H, m, CHO, cholesteryl), 5.42 (1 H, m, C=CH, cholesteryl), 6.83 [2 H, d, aromatic H (benzoyl)], 7.43 [2 H, d, aromatic H (L)], 7.66 [2 H, d, aromatic H (L)] and 7.94 [2 H, d, aromatic H (benzoyl)]; $\delta_C(CDCl_3)$ 63.96 ($OCH_2$), 66.92 ($OCH_2$), 113.97 (aromatic CCN), 114.58 [2 C, aromatic CH (benzyl)], 117.81 (PhCN), 124.40 (aromatic $CCO_2$), 127.63 [2 C, aromatic CH (L)], 131.76 (aromatic CNC), 132.21 [2 C, aromatic CH (benzoyl)], 134.26 [2 C, aromatic CH (L)], 162.77 (aromatic CO), 163.79 (PhNC), 166.29 ($CO_2$ of cholesteryl), 180.56 ($CO_2CH_2$), 200.74 (8 C, CO), 252.03 ($CCo_3$) and 12.55, 19.42. 20.06, 21.75, 23.24, 23.49, 24.53, 24.99, 28.64, 28.70, 28.92, 32.60, 32.62, 36.49, 36.89, 37.36, 37.75, 38.98, 40.21, 40.46, 43.03, 50.77, 56.86, 57.41, 75.04, 123.40 and 140.43 (27 C, cholesteryl).

$[Co_3(CO)_8(CCO_2Me)(CNC_6H_4CN)]$ **4**. This compound was obtained by reaction of tricobalt cluster **5** (500 mg, 1.00 mmol) with isocyanide **VIII** (315 mg, 2.50 mmol) as described above for compound **1**. Separation by column chromatography (hexane–$CH_2Cl_2$–$Et_2O$, 4:1:1) gave unreacted **5** (70%), which eluted first, followed by cluster **4** (23%) and then by polysubstituted clusters. Recrystallization from hexane–$CH_2Cl_2$ at −20 °C afforded pure **4** (134 mg, 22%) as a purple *solid*, $R_f$ ($Et_2O$–hexane, 1:1) 0.36, m.p. < 50 °C (decomp.) (Found: C, 37.9; H, 1.2; N, 4.6. $C_{19}H_7Co_3N_2O_{10}$ requires C, 38.0; H, 1.2; N, 4.7%); $\nu_{max}(CH_2Cl_2)$ 2236m, 2144s, 2088vs and 2055 (sh) $cm^{-1}$; $\delta_H(CDCl_3)$ 3.87 (3 H, s, $CH_3$), 7.49 (2 H, d, aromatic H) and 7.72 (2 H, d, aromatic H); $\delta_C(CDCl_3)$ 53.26 ($CH_3$), 113.92 (aromatic CCN), 117.90 (PhCN), 127.69 (2 C, aromatic CH), 131.87 (aromatic CNC), 134.30 (2 C, aromatic CH), 164.18 (PhNC), 181.24 ($CO_2$), 200.85 (8 C, CO) and 253.47 ($CCo_3$).

## Acknowledgements

One of the authors (R. D.) would like to thank the Swiss National Science Foundation for financial support (grants 21-27'581.89 and 20-32'174.91) and CIBA (Marly, Switzerland) for the elemental analyses. We thank the referees for helpful comments.

## References

1 H. Kuhn, *Thin Solid Films*, 1989, **178**, 1; *Langmuir–Blodgett Films*, ed. G. Roberts, Plenum, New York, 1990; B. Tieke, *Adv. Mater.*, 1990, **2**, 222.
2 H. Ringsdorf, B. Schlarb and S. Venzma, *Angew. Chem., Int. Ed. Engl.*, 1988, **27**, 113; A. Barraud, *Thin Solid Films*, 1989, **175**, 73.
3 R. H. Tredgold, *Rep. Prog. Phys.*, 1987, **50**, 1609.
4 R. Jones, R. H. Tredgold, A. Hoorfar and P. Hodge, *Thin Solid Films*, 1984, **113**, 115; E. Tsuchida, H. Nishida, M. Yuasa, T. Babe and M. Fukuzumi, *Macromolecules*, 1989, **22**, 66.
5 A. W. Snow, W. A. Barger, M. Klusty, H. Wohltjen and N. L. Jarvis, *Langmuir*, 1986, **2**, 513; M. J. Cook, A. J. Dunn, M. F. Daniel, R. C. O. Hart, R. M. Richardson and S. J. Roser, *Thin Solid Films*, 1988, **159**, 395; S. Palacin and A. Barraud, *J. Chem. Soc., Chem. Commun.*, 1989, 45; Y. Liu, K. Shigehara, M. Hara and A. Yamada, *J. Am. Chem. Soc.*, 1991, **113**, 440.
6 H. Nakahara, J. Nakayama, M. Hoshino and K. Fukuda, *Thin Solid Films*, 1988, **160**, 87.
7 Y. Nishikata, A. Morikawa, M. Kakimoto, Y. Imai, Y. Hirata, K. Nishiyama and M. Fujihira, *J. Chem. Soc., Chem. Commun.*, 1989, 1772; T. Murakata, T. Miyashita and M. Matsuda, *Macromolecules*, 1989, **22**, 2076; V. Cammarata, C. J. Kolaskie, L. L. Miller and B. J. Stallman, *J. Chem. Soc., Chem. Commun.*, 1990, 1290; F. Embs, D. Funhoff, A. Laschewsky, U. Licht, H. Ohst, W. Prass, H. Ringsdorf, G. Wegner and R. Wehrmann, *Adv. Mat.*, 1991, **3**, 25.
8 J. Li, M. Liu, H. Nakahara, M. Sato and K. Fukuda, *Chem. Lett.*, 1991, 101 and refs. therein.
9 T. Richardson, G. G. Roberts, M. E. C. Polywka and S. G. Davies, *Thin Solid Films*, 1988, **160**, 231; S. G. Davies, A. J. Smallridge, R. Colbrook, T. Richardson and G. G. Roberts, *J. Organomet. Chem.*, 1991, **401**, 181.
10 Y. Kawabata, M. Matsumoto, T. Nakamura, M. Tanaka, E. Manda, H. Takahashi, S. Tamura, W. Tagaki, H. Nakahara and K. Fukuda, *Thin Solid Films*, 1988, **159**, 353; H. Parrot-Lopez, C.-C. Ling, P. Zhang, A. Baszkin, G. Albrecht, C. de Rango and A. W. Coleman, *J. Am. Chem. Soc.*, 1992, **114**, 5479.
11 J. Malthête, D. Poupinet, R. Vilanove and J.-M. Lehn, *J. Chem. Soc., Chem. Commun.*, 1989, 1016.
12 M. A. Markowitz, R. Bielski and S. L. Regen, *J. Am. Chem. Soc.*, 1988, **110**, 7545.
13 P. N. Lindsay, B. M. Peake, B. H. Robinson, J. Simpson, U. Honrath, H. Vahrenkamp and A. M. Bond, *Organometallics*, 1984, **3**, 413 and refs. therein.
14 P. Lemoine, *Coord. Chem. Rev.*, 1988, **83**, 169.
15 P. Braunstein, *New J. Chem.*, 1986, **10**, 365.
16 D. Seyferth, G. H. Williams and C. L. Nievert, *Inorg. Chem.*, 1977, **16**, 758.
17 D. Seyferth, J. E. Hallgren and P. L. K. Hung, *J. Organomet. Chem.*, 1973, **50**, 265.
18 R. Obrecht, R. Herrmann and I. Ugi, *Synthesis*, 1985, 400.
19 W. D. S. Motherwell and W. Clegg, PLUTO, Program for plotting molecular and crystal structures, University of Cambridge, 1978.
20 P. W. Sutton and L. F. Dahl, *J. Am. Chem. Soc.*, 1967, **89**, 261.
21 K. Naito, A. Miura and M. Azuma, *J. Am. Chem. Soc.*, 1991, **113**, 6386.
22 (*a*) D. Hönig and D. Möbius, *J. Phys. Chem.*, 1991, **95**, 4590; (*b*) S. Henon and J. Meunier, *Rev. Sci. Instrum.*, 1991, **62**, 936.
23 (*a*) D. Hönig and D. Möbius, *Thin Solid Films*, 1992, **210/211**, 64; (*b*) D. Hönig, G. A. Overbeck and D. Möbius, *Adv. Mater.*, 1992, **4**, 419.
24 J. Adams, A. Buscke and R. S. Duran, *Macromolecules*, 1993, **26**, 2871.
25 G. Binnig, C. F. Quate and Ch. Gerber, *Phys. Rev. Lett.*, 1986, **56**, 930.
26 A. L. Weisenhorn, M. Egger, F. Ohnesorge, S. A. C. Gould, S.-P. Heyn, H. G. Hansma, R. L. Sinsheimer, H. E. Gaub and P. K. Hansma, *Langmuir*, 1991, **7**, 8; J. Frommer, *Angew. Chem., Int. Ed. Engl.*, 1992, **31** 1298.
27 A. L. Weisenhorn, D. U. Römer and G. P. Lorenzi, *Langmuir*, 1992, **8**, 3145.
28 A. P. Polishchuk, M. Yu. Antipin, T. V. Timofeeva, O. D. Lavrentovich, A. S. Kotel'chuk, L. A. Taraborkin and Yu. T. Struchkov, *Kristallografiya*, 1988, **33**, 1134.
29 E. J. Gabe, Y. Le Page, J.-P. Charland, F. L. Lee and P. S. White, *J. Appl. Crystallogr.*, 1989, **22**, 384.
30 *International Tables for X-Ray Crystallography*, Kynoch Press, Birmingham (Present distributor Kluwer Academic Publishers, Dordrecht), 1974, vol. 4.
31 M. T. Bogert and L. E. Wise, *J. Am. Chem. Soc.*, 1910, **32**, 1494.
32 I. Ugi, U. Fetzer, U. Eholzer, H. Knupfer and K. Offermann, *Angew. Chem.*, 1965, **77**, 492.

*Received* 1st *October* 1993; *Paper* 3/05918I